

Linear Response Theory for Shear Modulus C_{66} and Raman Quadrupole Susceptibility: Significant Evidence for Orbital Nematic Fluctuations in Fe-Based Superconductors

Hiroshi KONTANI and Youichi YAMAKAWA

Department of Physics, Nagoya University, Furo-cho, Nagoya 464-8602, Japan.

(Dated: November 10, 2018)

The emergence of the nematic order and fluctuations has been discussed as a central issue in Fe-based superconductors. To clarify the origin of the nematicity, we focus on the shear modulus C_{66} and the Raman quadrupole susceptibility $\chi_{x^2-y^2}^{\text{Raman}}$. Due to the Aslamazov-Larkin vertex correction, the nematic-type orbital fluctuations are induced, and they enhances both $1/C_{66}$ and $\chi_{x^2-y^2}^{\text{Raman}}$ strongly. However, $\chi_{x^2-y^2}^{\text{Raman}}$ remains finite even at the structure transition temperature T_S , because of the absence of the band Jahn-Teller effect and the Pauli (=intra-band) contribution, as proved in terms of the linear response theory. The present study clarifies that origin of the nematicity in Fe-based superconductors is the nematic-orbital order/fluctuations.

PACS numbers: 74.70.Xa, 74.20.-z, 74.20.Rp

In Fe-based superconductors, the nematic order and fluctuations attract great attention as one of the essential properties of the electronic states. A schematic phase diagram of BaFe_2As_2 as a function of carrier doping y is shown in Fig. 1: For $y > 0$ (e-doping), the non-magnetic orthorhombic (C_2) phase transition occurs at T_S , and the antiferro (AF) spin order is realized at T_N ($\lesssim T_S$) in the C_2 phase. In $\text{Ba}(\text{Fe}_{1-x}\text{Co}_x)_2\text{As}_2$ ($y = x$), both the structural and magnetic quantum critical points (QCPs) are very close, and strong magnetic fluctuations are observed near the QCPs by NMR [1]. In addition, strong nematic susceptibility that couples to the C_2 structure deformation had been observed via the softening of shear modulus C_{66} [2–6] and in-plane anisotropy of resistivity [7]. Similar softening of C_{66} is also observed in $(\text{Ba}_{1-x}\text{K}_x)\text{Fe}_2\text{As}_2$ ($y = -x/2$; h-doping) [5] and $\text{Fe}(\text{Se},\text{Te})$ ($y = 0$) [8]. Interestingly, in $\text{Ba}(\text{Fe}_{1-x}\text{Ni}_x)_2\text{As}_2$ ($y = 2x$), magnetic QCP and structural QCP are well separated, and quantum criticalities are realized at both points [9].

Then, a natural question is what is the “nematic order parameter” that would be closely related to the pairing mechanism. Up to now, both the spin-nematic mechanism [2] and ferro-orbital order mechanism [10–13] had been proposed, and the softening of C_{66} can be fitted by both mechanisms [14, 15]. The former predicts that the spin-nematic order $\langle \mathbf{s}_i \cdot \mathbf{s}_{i+\hat{x}} \rangle \neq 0$ occurs above T_N when the magnetic order $\langle \mathbf{s}_i \rangle$ is suppressed by the J_1 - J_2 frustration. As for the latter scenario, it was shown that the orbital order $n_{xz} \neq n_{yz}$ is induced by spin fluctuations, due to strong spin-orbital mode-coupling given by the vertex correction (VC) [13, 16, 17]. The large d -orbital level splitting $E_{yz} - E_{xz} \sim 60$ meV in the C_2 phase [18, 19] may be too large to be produced by spin nematic order via spin-lattice coupling.

Recently observed large quadrupole susceptibility $\chi_{x^2-y^2}^{\text{Raman}}$ by electron Raman spectroscopy [20, 21] presents a direct evidence of the strong orbital fluctuations. Although this result favors the orbital nematic scenario, the

observed enhancement of $\chi_{x^2-y^2}^{\text{Raman}}$ is apparently smaller than the orbital susceptibility extracted from C_{66} . For example, $\chi_{x^2-y^2}^{\text{Raman}}$ remains finite at $T = T_S$, although C_{66}^{-1} diverges at T_S . Therefore, it should be verified whether both C_{66} and $\chi_{x^2-y^2}^{\text{Raman}}$ can be explained based on the orbital nematic scenario or not.

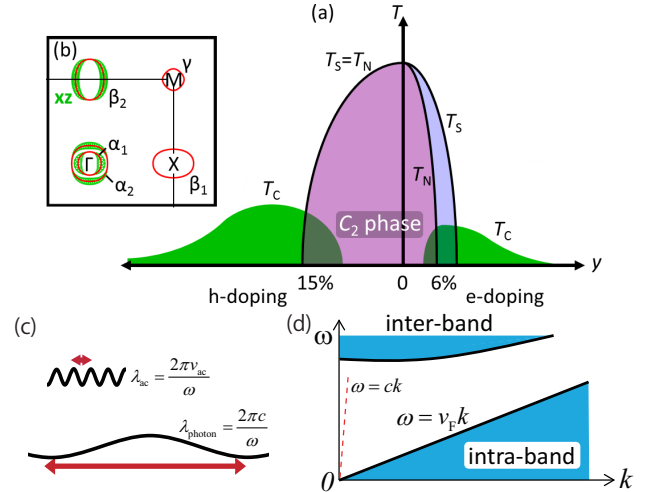


FIG. 1: (color online) (a) Schematic phase diagram of Fe-based superconductors. (b) Fermi surfaces for $y = 0$. The weight of d_{xz} orbital is stressed by green circles. (c) Relation $\lambda_{\text{photon}} \gg \lambda_{\text{ac}}$. (d) Particle-hole excitation continuum.

In this paper, we analyze both C_{66} and $\chi_{x^2-y^2}^{\text{Raman}}$, both of which are key experiments to uncover the nematic order parameter. It is found that both C_{66} and $\chi_{x^2-y^2}^{\text{Raman}}$ are enhanced by the orbital fluctuations due to Aslamazov-Larkin type VC (AL-VC). However, $\chi_{x^2-y^2}^{\text{Raman}}$ is less singular since the band Jahn-Teller (band-JT) effect and the Pauli (=intra-band) quadrupole susceptibilities does not contribute to $\chi_{x^2-y^2}^{\text{Raman}}$. Since both C_{66} and $\chi_{x^2-y^2}^{\text{Raman}}$ are explained satisfactorily, the orbital nematic scenario is essential for many Fe-based superconductors.

As for the pairing mechanism, at present, both the spin fluctuation mediated s_{\pm} wave state [22–24] and orbital fluctuation mediated s_{++} wave state [25, 26] have been discussed. When both fluctuations coexist, nodal s -wave state can be realized [27]. The s_{++} -wave state is consistent with the robustness of T_c against impurities [28, 29] and broad hump structure in the inelastic neutron scattering [30, 31]. The self-consistent vertex correction (SC-VC) method [13, 26] predicts the developments of ferro- and AF-orbital fluctuations, and the freezing of the latter fluctuations would explain the nematic order at $T^* \sim 200\text{K}$ ($\gg T_S$) [32, 33].

First, we discuss the susceptibility at $\mathbf{k} \approx \mathbf{0}$ with respect to the quadrupole order parameter $\hat{O}_{x^2-y^2} \equiv n_{xz} - n_{yz}$ in the Hubbard model. For $U = U' + 2J$, it is approximately given as [13, 16]

$$\chi_{x^2-y^2}(k) = 2\Phi(k)/(1 - (U - 5J)\Phi(k)), \quad (1)$$

where $k = (\mathbf{k}, \omega)$, and $\Phi(k) \equiv \chi^{(0)}(k) + X(k)$ is the intra-orbital (within d_{xz} orbital) irreducible susceptibility: $\chi^{(0)}(k)$ is the non-interacting susceptibility and $X(k)$ is the VC for the charge channel. The orbital nematic order $n_{xz} \neq n_{yz}$ occurs when the charge Stoner factor $\alpha_c = (U - 5J)\Phi(0)$ reaches unity, which is realized near the magnetic QCP since the AL-VC is proportional to the square of the magnetic correlation length [13, 16, 17].

Next, we discuss the “total” quadrupole susceptibility in real systems, by including the realistic quadrupole interaction due to the acoustic phonon for the orthorhombic distortion. According to Ref. [34], it is given as $-g_{ac}(k)\hat{O}_{x^2-y^2}(\mathbf{k})\hat{O}_{x^2-y^2}(-\mathbf{k})$, where $\hat{O}_{x^2-y^2}(\mathbf{k})$ is the quadrupole operator, and $g_{ac}(k) = g \cdot (v_{ac}|\mathbf{k}/\omega|)^2 / ((v_{ac}|\mathbf{k}/\omega|)^2 - 1)$ is the phonon propagator multiplied by the coupling constants. v_{ac} is the phonon velocity. Since the Migdal’s theorem tells that the effect of g on the irreducible susceptibility is negligible, the total susceptibility is

$$\chi_{x^2-y^2}^{\text{tot}}(k) = \chi_{x^2-y^2}(k)/(1 - g_{ac}(k)\chi_{x^2-y^2}(k)). \quad (2)$$

Now, we discuss the acoustic and optical responses based on the total susceptibility (2), by taking notice that any susceptibilities in metals are *discontinuous* at $\omega = |\mathbf{k}| = 0$. Since the elastic constant is measured under the static ($\omega = 0$) strain with long wavelength ($|\mathbf{k}| \rightarrow 0$), C_{66} is given as

$$C_{66}^{-1} \sim 1 + \lim_{\mathbf{k} \rightarrow \mathbf{0}} g_{ac}(\mathbf{k}, 0)\chi_{x^2-y^2}^{\text{tot}}(\mathbf{k}, 0) = \frac{1}{1 - g\chi_{k\text{-lim}}}, \quad (3)$$

where $\chi_{k\text{-lim}} \equiv \lim_{\mathbf{k} \rightarrow \mathbf{0}} \chi_{x^2-y^2}(\mathbf{k}, 0)$ is called the k -limit, and the relation $g_{ac}(k) = g$ for $\omega = 0$ is taken into account. The structure transition occurs when C_{66}^{-1} diverges. When the AL-VC is negligible, $\chi_{k\text{-lim}}$ is as small as $\chi_{k\text{-lim}}^{(0)}$. Even in this case, C_{66}^{-1} can diverge when g is very large, which is known as the band-JT effect. However, the band-JT mechanism cannot explain the strong

enhancement of $\chi_{x^2-y^2}^{\text{Raman}}$, as we will clarify later. In fact, the fitting of experimental data in the present paper indicates that the softening of C_{66} is mainly given by the AL-VC: The relation $1/g \sim \chi_{k\text{-lim}} \gg \chi_{k\text{-lim}}^{(0)}$ is satisfied in Fe-based superconductors.

Next, we derive the optical response in the DC limit, measured by using the low-energy photon with $k = (\mathbf{k}, \omega = c|\mathbf{k}|)$ and $\omega \rightarrow 0$. Considering that the photon velocity c is much faster than the Fermi velocity v_F and v_{ac} , it is given as

$$\chi_{x^2-y^2}^{\text{Raman}} \sim \lim_{\omega \rightarrow 0} \chi_{x^2-y^2}^{\text{tot}}(\mathbf{0}, \omega) = \chi_{\omega\text{-lim}}, \quad (4)$$

where $\chi_{\omega\text{-lim}} \equiv \lim_{\omega \rightarrow 0} \chi_{x^2-y^2}(\mathbf{0}, \omega)$ is called the ω -limit [35, 36]. Since $g_{ac}(k)$ is zero for $|\omega/\mathbf{k}| = c$, the band-JT effect does not contribute to the Raman susceptibility. The physical explanation is that the acoustic phonons cannot be excited by photons because of the mismatch of the wavelengths $\lambda_{\text{photon}} \gg \lambda_{\text{ac}}$ for the same ω as shown in Fig. 1 (c). Also, since $c \gg v_F$, low-energy photon cannot induce the intraband particle-hole excitation as understood from the location of the particle-hole continuum shown in Fig. 1 (d). This fact leads to the relationship “ $\chi_{\omega\text{-lim}}$ is smaller than $\chi_{k\text{-lim}}$ ” as we discuss mathematically later. For the charge quadrupole susceptibility, this relationship holds even if the quasiparticle lifetime is finite due to impurity scattering; see the Supplemental Material [37]. Therefore, $\chi_{x^2-y^2}^{\text{Raman}}$ remains finite at $T \sim T_S$ although C_{66}^{-1} diverges at T_S , consistently with experiments [20, 21].

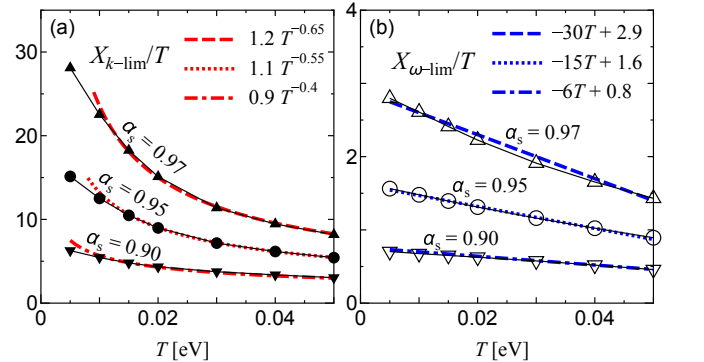


FIG. 2: (color online) (a) $X_{k\text{-lim}}/T$ and (b) $X_{\omega\text{-lim}}/T$ as functions of T . Their T -dependences originates from $|\Lambda_Q^{k(\omega)\text{-lim}}|^2$ since $\xi^2 \propto 1/(1 - \alpha_s)$ is fixed.

Hereafter, we perform the numerical calculation of the quadrupole susceptibility in the five-orbital model. The unit of energy is eV unless otherwise noted. First, we discuss the k -limit and ω -limit of the bare bubble made of two d_{xz} -orbital Green functions. They are connected by the following relation:

$$\chi_{k\text{-lim}}^{(0)} = \chi_{\omega\text{-lim}}^{(0)} + \sum_{\alpha}^{\text{band}} \left(-\frac{\partial f_{\mathbf{k}}^{\alpha}}{\partial \epsilon_{\mathbf{k}}^{\alpha}} \right) \{z_{\mathbf{k}}^{\alpha}\}^2, \quad (5)$$

where $z_{\mathbf{k}}^{\alpha} = |\langle xz, \mathbf{k} | \alpha, \mathbf{k} \rangle|^2 \leq 1$ is the weight of the d_{xz} -orbital on band α , and $f_{\mathbf{k}}^{\alpha} = (\exp((\epsilon_{\mathbf{k}}^{\alpha} - \mu)/T) + 1)^{-1}$.

In Eq. (5), $\chi_{\omega\text{-lim}}^{(0)} = \sum_{\alpha \neq \beta}^{\text{band}} \frac{f_{\mathbf{k}}^{\alpha} - f_{\mathbf{k}}^{\beta}}{\epsilon_{\mathbf{k}}^{\beta} - \epsilon_{\mathbf{k}}^{\alpha}} z_{\mathbf{k}}^{\alpha} z_{\mathbf{k}}^{\beta}$ is given by only the inter-band ($\alpha \neq \beta$) contribution, which is called the Van-Vleck term. Therefore, $\chi_{k\text{-lim}}^{(0)}$ is always larger than $\chi_{\omega\text{-lim}}^{(0)}$ due to the intra-band contribution given by the second term in Eq. (5), called the Pauli term. We obtain $\chi_{\omega\text{-lim}}^{(0)} \approx 0.25$ and $\chi_{k\text{-lim}}^{(0)} \approx 0.45$ in the present model.

Next, we analyze AL-VC in detail, since it is the main driving force of the orbital fluctuations. The analytic expression of the AL term is given in Refs. [13, 16]. To simplify the discussion, we consider the intra-orbital (within d_{xz} -orbital) AL-term. Then, $X_{k(\omega)\text{-lim}}$ is approximately given as

$$X_{k(\omega)\text{-lim}} = 3T \sum_{\mathbf{q}} |\Lambda_{\mathbf{q}}^{k(\omega)\text{-lim}}|^2 V^s(\mathbf{q}, 0)^2, \quad (6)$$

where $\Lambda_{\mathbf{q}}^{\omega\text{-lim}} \equiv \lim_{\omega \rightarrow 0} \Lambda_{\mathbf{q}}(\mathbf{0}, \omega)$ and $\Lambda_{\mathbf{q}}^{k\text{-lim}} \equiv \lim_{\mathbf{k} \rightarrow \mathbf{0}} \Lambda_{\mathbf{q}}(\mathbf{k}, 0)$ at $\mathbf{q} = (\mathbf{q}, 0)$: $\Lambda_{\mathbf{q}}(\mathbf{k}, 0)$ is the three-point vertex made of three Green functions [13]. Also, $V^s(\mathbf{q}) = U + U^2 \chi^s(\mathbf{q})$, where $\chi^s(\mathbf{q})$ is the spin susceptibility for d_{xz} -orbital. Here, we assume the following Millis-Monien-Pines form of $\chi^s(\mathbf{q})$ [38]:

$$\chi^s(\mathbf{q}) = c\xi^2(1 + \xi^2(\mathbf{q} - \mathbf{Q})^2 + |\Omega_m|/\omega_{\text{sf}})^{-1}, \quad (7)$$

where $\mathbf{Q} = (0, \pm\pi)$, $\xi^2 = l/(T - \theta)$ is the square of the spin correlation length, and $\omega_{\text{sf}} = l'\xi^{-2}$ is the spin-fluctuation energy scale. Quantitatively speaking, $X_{k(\omega)\text{-lim}}$ given by Eq. (6) is underestimated since non-zero Matsubara terms are dropped. However, in the classical region $\omega_{\text{sf}} < 2\pi T$, which is realized in optimally-doped $\text{Ba}(\text{Fe}, \text{Co})_2\text{As}_2$ [39], $\chi^s(\mathbf{q}, \omega_l)$ for $l \neq 0$ is negligibly small. In this case, we can safely use Eq. (6).

According to Eqs. (6) and (7), we obtain $X_{k(\omega)\text{-lim}} \sim T \{ \Lambda_{\mathbf{Q}}^{k(\omega)\text{-lim}} \}^2 \xi^2$ for two-dimensional systems. $\Lambda_{\mathbf{Q}}^{k\text{-lim}}$ and $\Lambda_{\mathbf{Q}}^{\omega\text{-lim}}$ are connected by the following relation:

$$\Lambda_{\mathbf{Q}}^{k\text{-lim}} = \Lambda_{\mathbf{Q}}^{\omega\text{-lim}} + \sum_{\alpha, \gamma} \sum_{\mathbf{k}} \left(-\frac{\partial f_{\mathbf{k}}^{\alpha}}{\partial \epsilon_{\mathbf{k}}^{\alpha}} \right) \frac{\{z_{\mathbf{k}}^{\alpha}\}^2 z_{\mathbf{k}-\mathbf{Q}}^{\gamma}}{\epsilon_{\mathbf{k}-\mathbf{Q}}^{\gamma} - \epsilon_{\mathbf{k}}^{\alpha}}, \quad (8)$$

where $\Lambda_{\mathbf{Q}}^{\omega\text{-lim}}$ is the inter-band Van-Vleck term [40]. For $\mathbf{q} \approx \mathbf{Q}$, $\Lambda_{\mathbf{Q}}^{k\text{-lim}}$ increases strongly at low T , because of the intra-band ‘‘Pauli term’’ in the second term of Eq. (8). Its main contribution is given by $\alpha = \alpha_{1,2}$ and $\gamma = \beta_2$ in Fig. 1 (b). Both Pauli and Van-Vleck terms are negative in the present model. Therefore, the relationship $X_{k\text{-lim}} > X_{\omega\text{-lim}}$ is satisfied.

Figure 2 (a) shows the temperature dependence of $X_{k\text{-lim}}/T$ given by Eq. (6), by using the static RPA spin susceptibility $\chi^s(\mathbf{q}, 0)$ obtained at $T = 0.01$. In this calculation, $\xi^2 \propto (1 - \alpha_s)^{-1}$ is fixed, where $\alpha_s = U\chi^{(0)}(\mathbf{Q}, 0)$

is the spin Stoner factor. Thus, we obtain the relationship $X_{k\text{-lim}}/T \sim T^{-0.5}\xi^2$, in which the factor $T^{-0.5}$ originates from the strong T -dependence of $|\Lambda_{\mathbf{Q}}^{k\text{-lim}}|^2$. We also show the temperature dependence of $X_{\omega\text{-lim}}/T$ in Fig. 2 (b): The relation $X_{\omega\text{-lim}}/T \sim (b - T)\xi^2$ is realized due to the T -dependence of $|\Lambda_{\mathbf{Q}}^{\omega\text{-lim}}|^2$ [40]. Therefore, the relationship $X_{k\text{-lim}} > X_{\omega\text{-lim}}$ is confirmed by the present calculation.

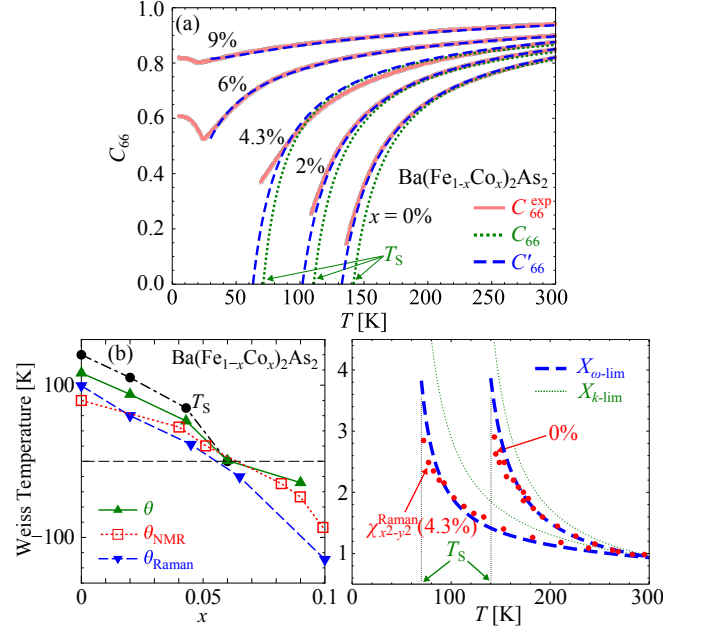


FIG. 3: (color online) (a) Fittings of the data C_{66}^{exp} normalized by the 33% Co-Ba122 data in Ref. [5], shown by broad red lines. The dotted lines C_{66} is the fitting result under the constraint $C_{66} = 0$ at $T = T_s$, and the broken lines C_{66}' is the fitting without constraint. (b) The Weiss temperature θ given by the present fitting. θ_{NMR} is the Weiss temperature of $1/T_1 T$ [1], and θ_{Raman} is given by the Raman spectroscopy [20]. (c) $X_{k\text{-lim}}$ and $X_{\omega\text{-lim}}$ given by the fitting of C_{66} . Experimental data of $\chi_{x^2-y^2}^{\text{Raman}}$ are shown by red circles [20].

Here, we perform the fitting of experimental data. To reduce the number of fitting parameters, we put $\chi_{x^2-y^2} \approx 2\Phi$ by assuming $(U - 5J) \sim 0$, which would be justified since the relation $J/U \sim 0.15$ is predicted by the first principle study [41]. Also, we put $\Phi \approx X$ by assuming that $X \gg \chi^{(0)}$. Then, Eqs. (3) and (4) are simplified as

$$C_{66}^{-1} \propto 1/(1 - 2gX_{k\text{-lim}}), \quad (9)$$

$$\chi_{x^2-y^2}^{\text{Raman}} \propto X_{\omega\text{-lim}}, \quad (10)$$

where $X_{k\text{-lim}} \equiv a_0 T^a \xi^2$ and $X_{\omega\text{-lim}} \equiv b_0 (b - T) T \xi^2$: According to Fig.2, $a \sim 0.5$ and $b \sim 0.1$ for $T > 0.01$.

First, we fit the data of C_{66}^{exp} , which is normalized by the shear modulus due to phonon anharmonicity (=33% Co-Ba122 data) given in Ref. [5]. We putting $a = 0.5$, and the remaining fitting parameters are $h = 2ga_0 l$ and θ . Figure 3 (a) shows the fitting result for

Ba(Fe_{1-x}Co_x)₂As₂: The “dotted line C_{66} ” is the fitting result of C_{66}^{exp} under the constraint $C_{66} = 0$ at $T = T_S$. We fix $h = 2.16$ for all x , and change θ from 116K to -30 K. The “broken line C'_{66} ” is the fitting for $x = 0 \sim 0.09$ without the constraint, by using $h = 2.67$. Thus, both fitting methods can fit the T - and x -dependences of C_{66}^{exp} very well by choosing only $\theta(x)$ with a fixed h . Figure 3 (b) shows the obtained $\theta(x)$ by C_{66} -fitting ($x = 0 \sim 0.043$) and by C'_{66} -fitting ($x = 0.06, 0.09$), as explained above. The obtained $\theta(x)$ is very close to θ_{NMR} given by the Curie-Weiss fitting of $1/T_1T$ [1], which manifests the importance of the AL-VC. Also, θ_{Raman} is given by the Raman spectroscopy [20].

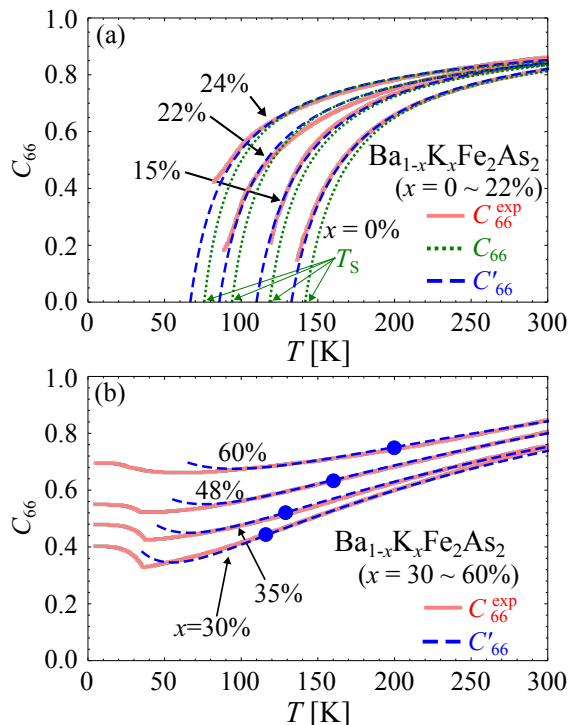


FIG. 4: (color online) Fittings of shear modulus for (a) under-doped and (b) over-doped (Ba_{1-x}K_x)Fe₂As₂. Experimental data C_{66}^{exp} are shown by broad red lines [5].

In Fig. 3 (c), we show $X_{k\text{-lim}}$ obtained by the fitting of C_{66}^{exp} for Ba(Fe_{1-x}Co_x)₂As₂ at $x = 0$ and 0.043. We also show $X_{\omega\text{-lim}} \sim X_{k\text{-lim}} \cdot (b - T)T^{1-a}$ according to the numerical result in Fig. 2, by putting $b = 1400$ K. In Fig. 3 (c), all the data are normalized as unity at 300K. Then, the relation $\chi_{x^2-y^2}^{\text{Raman}} \sim X_{\omega\text{-lim}}$ is well satisfied, as expected from Eq. (10). In addition, the relation $X_{\omega\text{-lim}} \ll X_{k\text{-lim}}$ holds for $T \sim T_S$, consistently with the report in Ba(Fe_{1-x}Co_x)₂As₂ [20].

Figure 4 (a) and (b) shows the fitting results for (Ba_{1-x}K_x)Fe₂As₂ for $x = 0 \sim 0.24$ ($a = 0.5$; $h = 2.16$ for C_{66} and $h = 2.67$ for C'_{66}) and $x = 0.3 \sim 0.6$ ($a = 0.58$; $h = 4.98$ for C'_{66}), respectively. In the present theory, we can explain the existence of inflection points of C_{66} in over-doped region (without structure transition) re-

ported experimentally [5], shown by large blue circles. The inflection point originates from the factor T^a in $X_{k\text{-lim}} \propto T^a \xi^2$. The fitting of over-doped data could be improved by considering the deviation from the relation $X_{k\text{-lim}} \propto T^a \xi^2$ at low T , as recognized in Fig. 2 (a). In addition, for $x \gtrsim 0.5$, experimental pseudo-gap behavior of $1/T_1T$ ($\propto \xi^2$) below ~ 100 K [42] would also be related to the inflection point of C_{66} .

In the present theory, we can fit C_{66}^{exp} very well for both over-doped and under-doped regions in Ba_{1-x}K_xFe₂As₂. However, different set of parameters should be used in each region: This fact indicates that the orthorhombic phase and superconducting phase are separated by the first-order transition. In fact, the T^2 -like resistivity at the optimum doping $x \sim 0.3$ indicates the absence of the orbital-nematic QCP in this compound. We also note that the change in the topology of the electron-pockets, called the Lifshitz transition, occurs in Ba_{1-x}K_xFe₂As₂ near the optimal doping.

In this paper, we showed that Raman susceptibility at $\omega = 0$ is enlarged by the AL-VC. The present theory predicts that the ω -dependence of the AC Raman susceptibility follows $\chi_{x^2-y^2}^{\text{Raman}}(\omega) \sim X(\mathbf{0}, \omega) \sim (1 - i\omega/\Gamma)^{-1}$, and Γ is approximately $\sim \omega_{\text{sf}}$. However, Γ could be modified by the ω -dependence of $|\Lambda_q(k)|^2$.

In summary, we presented a unified explanation for the softening of C_{66} and enhancement of $\chi_{x^2-y^2}^{\text{Raman}}$ based on the five-orbital model. Both $1/C_{66}$ and $\chi_{x^2-y^2}^{\text{Raman}}$ are enhanced by the nematic-type orbital fluctuations induced by the AL-VC. However, $\chi_{x^2-y^2}^{\text{Raman}}$ remains finite even at the structure transition temperature T_S , because of the absence of the band-JT effect and the Pauli (=intra-band) contribution. The present study clarified that the origin of the nematicity, which is a central issue in Fe-based superconductors, is the nematic-orbital order/fluctuations.

We are grateful to A.E. Böhmer for offering us her experimental data published in Ref. [5]. We also thank Y. Gallais, A.V. Chubukov, J. Schmalian, R. Fernandes and S. Onari for useful discussions. This study has been supported by Grants-in-Aid for Scientific Research from MEXT of Japan. Part of numerical calculations were performed on the Yukawa Institute Computer Facility.

-
- [1] F. L. Ning, K. Ahilan, T. Imai, A. S. Sefat, M. A. McGuire, B. C. Sales, D. Mandrus, P. Cheng, B. Shen, and H.-H. Wen, Phys. Rev. Lett. **104**, 037001 (2010)
 - [2] R.M. Fernandes, L. H. VanBebber, S. Bhattacharya, P. Chandra, V. Keppens, D. Mandrus, M.A. McGuire, B.C. Sales, A.S. Sefat, and J. Schmalian, Phys. Rev. Lett. **105**, 157003 (2010).
 - [3] M. Yoshizawa, D. Kimura, T. Chiba, S. Simayi, Y. Nakanishi, K. Kihou, C.-H. Lee, A. Iyo, H. Eisaki, M. Nakajima, and S. Uchida, J. Phys. Soc. Jpn. **81**, 024604

- (2012).
- [4] S. Simayi, K. Sakano, H. Takezawa, M. Nakamura, Y. Nakanishi, K. Kihou, M. Nakajima, C.-H. Lee, A. Iyo, H. Eisaki, S. Uchida, and M. Yoshizawa, *J. Phys. Soc. Jpn.* **82**, 114604 (2013).
- [5] A. E. Böhrer, P. Burger, F. Hardy, T. Wolf, P. Schweiss, R. Fromknecht, M. Reinecker, W. Schranz, and C. Meingast, *Phys. Rev. Lett.* **112**, 047001 (2014).
- [6] T. Goto, R. Kurihara, K. Araki, K. Mitsumoto, M. Akatsu, Y. Nemoto, S. Tatematsu, and M. Sato, *J. Phys. Soc. Jpn.* **80**, 073702 (2011).
- [7] H.-H. Kuo, J. G. Analytis, J.-H. Chu, R. M. Fernandes, J. Schmalian, and I. R. Fisher, *Phys. Rev. B* **86**, 134507 (2012).
- [8] M. Yoshizawa, private communication.
- [9] R. Zhou, Z. Li, J. Yang, D. L. Sun, C. T. Lin, and G. Zheng, *Nat. Commun* **4**, 2265, (2013).
- [10] F. Krüger, S. Kumar, J. Zaanen, J. van den Brink, *Phys. Rev. B* **79**, 054504 (2009).
- [11] W. Lv, J. Wu and P. Phillips, *Phys. Rev. B* **80**, 224506 (2009); W. Lv, F. Kruger, and P. Phillips, *Phys. Rev. B* **82**, 045125 (2010).
- [12] C.-C. Lee, W.-G. Yin, and W. Ku, *Phys. Rev. Lett.* **103**, 267001 (2009)
- [13] S. Onari and H. Kontani, *Phys. Rev. Lett.* **109**, 137001 (2012).
- [14] H. Kontani, Y. Inoue, T. Saito, Y. Yamakawa and S. Onari, *Solid State Communications*, **152**, 718 (2012).
- [15] R.M. Fernandes and A.J. Millis, *Phys. Rev. Lett.* **111**, 127001 (2013).
- [16] Y. Ohno, M. Tsuchiizu, S. Onari, and H. Kontani, *J. Phys. Soc. Jpn.* **82**, 013707 (2013).
- [17] M. Tsuchiizu, Y. Ohno, S. Onari and H. Kontani, *Phys. Rev. Lett.* **111**, 057003 (2013).
- [18] M. Yi, D. H. Lu, J.-H. Chu, J. G. Analytis, A. P. Sorini, A. F. Kemper, B. Moritz, S.-K. Mo, R. G. Moore, M. Hashimoto, W.-S. Lee, Z. Hussain, T. P. Devereaux, I. R. Fisher, and Z.-X. Shen, *Proc. Natl. Acad. Sci. USA* **108**, 6878 (2011).
- [19] H. Miao, L.-M. Wang, P. Richard, S.-F. Wu, J. Ma, T. Qian, L.-Y. Xing, X.-C. Wang, C.-Q. Jin, C.-P. Chou, Z. Wang, W. Ku, and H. Ding, arXiv:1310.4601
- [20] Y. Gallais, R. M. Fernandes, I. Paul, L. Chauviere, Y.-X. Yang, M.-A. Measson, M. Cazayous, A. Sacuto, D. Colson, and A. Forget, *Phys. Rev. Lett.* **111**, 267001 (2013).
- [21] Y.-X. Yang, Y. Gallais, R. M. Fernandes, I. Paul, L. Chauviere, M.-A. Measson, M. Cazayous, A. Sacuto, D. Colson, and A. Forget arXiv:1310.0934
- [22] K. Kuroki, S. Onari, R. Arita, H. Usui, Y. Tanaka, H. Kontani, and H. Aoki, *Phys. Rev. Lett.* **101**, 087004 (2008).
- [23] P. J. Hirschfeld, M. M. Korshunov, I. I. Mazin *Rep. Prog. Phys.* **74**, 124508 (2011).
- [24] A. V. Chubukov, D. V. Efremov, and I. Eremin, *Phys. Rev. B* **78**, 134512 (2008).
- [25] H. Kontani and S. Onari, *Phys. Rev. Lett.* **104**, 157001 (2010).
- [26] S. Onari, Y. Yamakawa and H. Kontani, *Phys. Rev. Lett.* **112**, 187001 (2014).
- [27] T. Saito, S. Onari and H. Kontani, *Phys. Rev. B* **88**, 045115 (2013).
- [28] S. Onari and H. Kontani, *Phys. Rev. Lett.* **103**, 177001 (2009).
- [29] Y. Yamakawa, S. Onari, and H. Kontani, *Phys. Rev. B* **87**, 195121 (2013).
- [30] S. Onari, H. Kontani and M. Sato, *Phys. Rev. B* **81**, 060504(R) (2010)
- [31] S. Onari and H. Kontani, *Phys. Rev. B* **84**, 144518 (2011)
- [32] S. Kasahara, H. J. Shi, K. Hashimoto, S. Tonegawa, Y. Mizukami, T. Shibauchi, K. Sugimoto, T. Fukuda, T. Terashima, A. H. Nevidomskyy, and Y. Matsuda, *Nature* **486**, 382 (2012).
- [33] Y. K. Kim, W. S. Jung, G. R. Han, K.-Y. Choi, C.-C. Chen, T. P. Devereaux, A. Chainani, J. Miyawaki, Y. Takata, Y. Tanaka, M. Oura, S. Shin, A. P. Singh, H. G. Lee, J.-Y. Kim, and C. Kim, *Phys. Rev. Lett.* **111**, 217001 (2013).
- [34] H. Kontani, T. Saito and S. Onari, *Phys. Rev. B* **84**, 024528 (2011).
- [35] P. Nozieres, *Theory of Interacting Fermi Systems* (Benjamin, New York, 1964); A. A. Abrikosov, L. P. Gorkov and I. E. Dzyaloshinski, *Methods of Quantum Field Theory in Statistical Physics* Dover, New York, 1975); A. J. Leggett, *Phys. Rev.* **140**, A1869 (1965).
- [36] H. Kontani, and K. Yamada, *J. Phys. Soc. Jpn.* **65**, 172 (1996); H. Kontani, and K. Yamada, *J. Phys. Soc. Jpn.* **66**, 2232 (1997).
- [37] H. Kontani and Y. Yamakawa, Supplemental Material
- [38] A.-J. Millis, H. Monien and D. Pines, *Phys. Rev. B* **42**, 167 (1990); P. Monthoux and D. Pines, *Phys. Rev. B* **47**, 6069 (1993).
- [39] P. Steffens, C.H. Lee, N. Qureshi, K. Kihou, A. Iyo, H. Eisaki, and M. Braden, *Phys. Rev. Lett.* **110**, 137001 (2013).
- [40] The analytic expression of $\Lambda_q^{\omega\text{-lim}}$ is given as
- $$\Lambda_q^{\omega\text{-lim}} = \sum_{\alpha, \beta, \gamma}^{\alpha \neq \beta} \sum_{\mathbf{k}} \left\{ \frac{1}{\epsilon_{\mathbf{k}}^{\beta} - \epsilon_{\mathbf{k}}^{\alpha}} \left(\frac{f_{\mathbf{k}}^{\beta}}{\epsilon_{\mathbf{k}}^{\beta} - \epsilon_{\mathbf{k}-\mathbf{q}}^{\gamma}} - \frac{f_{\mathbf{k}}^{\alpha}}{\epsilon_{\mathbf{k}}^{\alpha} - \epsilon_{\mathbf{k}-\mathbf{q}}^{\gamma}} \right) + \frac{f_{\mathbf{k}-\mathbf{q}}^{\gamma}}{(\epsilon_{\mathbf{k}-\mathbf{q}}^{\gamma} - \epsilon_{\mathbf{k}}^{\alpha})(\epsilon_{\mathbf{k}-\mathbf{q}}^{\gamma} - \epsilon_{\mathbf{k}}^{\beta})} \right\} z_{\mathbf{k}}^{\alpha} z_{\mathbf{k}}^{\beta} z_{\mathbf{k}-\mathbf{q}}^{\gamma} + \sum_{\alpha, \gamma} \sum_{\mathbf{k}} \frac{f_{\mathbf{k}-\mathbf{q}}^{\gamma} - f_{\mathbf{k}}^{\alpha}}{(\epsilon_{\mathbf{k}}^{\alpha} - \epsilon_{\mathbf{k}-\mathbf{q}}^{\gamma})^2} \{z_{\mathbf{k}}^{\alpha}\}^2 z_{\mathbf{k}-\mathbf{q}}^{\gamma}.$$
- [41] T. Miyake, K. Nakamura, R. Arita and M. Imada, *J. Phys. Soc. Jpn.* **79**, 044705 (2010).
- [42] M. Hirano, Y. Yamada, T. Saito, R. Nagashima, T. Konishi, T. Toriyama, Y. Ohta, H. Fukazawa, Y. Kohori, Y. Furukawa, K. Kihou, C.-H. Lee, A. Iyo, and H. Eisaki, *J. Phys. Soc. Jpn.*, **81**, 054704 (2012).

**[SUPPLEMENTAL MATERIAL]: RELATIONSHIP
 $\chi_{k\text{-lim}} > \chi_{\omega\text{-lim}}$ IN THE PRESENCE OF
 IMPURITIES**

In the main text, we have studied the k -limit and ω -limit of the quadrupole susceptibility $\chi_{x^2-y^2}(\mathbf{q}, \omega)$, and found that the relationship $\chi_{k\text{-lim}} > \chi_{\omega\text{-lim}}$ is satisfied. The basis of this relationship is that the intraband Pauli term is absent in both $\chi_{\omega\text{-lim}}^{(0)}$ and $X_{\omega\text{-lim}} \sim T \sum_{\mathbf{q}} |\Lambda_{\mathbf{q}}^{\omega\text{-lim}}|^2 V^s(\mathbf{q})^2$ in the absence of the elastic and inelastic scattering. However, the relationship $\chi_{k\text{-lim}} > \chi_{\omega\text{-lim}}$ is not trivial when the scattering processes exist. Here, we calculate both $\chi_{\omega\text{-lim}}^{(0)}$ and $\Lambda_{\mathbf{q}}^{\omega\text{-lim}}$ in the presence of the local nonmagnetic impurities based on the T -matrix approximation in the five-orbital model. For the charge quadrupole susceptibility, the relationship $\chi_{k\text{-lim}} > \chi_{\omega\text{-lim}}$ is confirmed even in the presence of impurities.

We assume that the impurity potential I is diagonal in the orbital basis. (We write d_{z^2} , d_{xz} , d_{yz} , d_{xy} , $d_{x^2-y^2}$ orbitals as 1, 2, \dots , 5, respectively.) Then, the T -matrix in the orbital basis is given as

$$\hat{T}(\epsilon_n) = I(\hat{1} - I \sum_{\mathbf{q}} \hat{G}(\mathbf{q}, \epsilon_n))^{-1} \quad (11)$$

where $\epsilon_n = (2n+1)\pi T$ and the Green function is $\hat{G}(\mathbf{q}, \epsilon_n) = (i\epsilon_n + \mu - \hat{H}_{\mathbf{q}}^0 - \Sigma^{\text{imp}}(\epsilon_n))^{-1}$, and

$$\Sigma^{\text{imp}}(\epsilon_n) \equiv n_{\text{imp}} \hat{T}(\epsilon_n) \quad (12)$$

is the impurity self-energy when the impurity concentration is $n_{\text{imp}} (\ll 1)$. The Bethe-Salpeter equation for the one-particle operator \hat{O} is

$$\begin{aligned} \hat{L}^{\text{imp}}(k; \epsilon_n) &= \hat{O} + n_{\text{imp}} \sum_{\mathbf{q}} \hat{T}(\omega_l + \epsilon_n) \hat{G}(k+q) \\ &\quad \times \hat{L}^{\text{imp}}(k; \epsilon_n) \hat{G}(q) \hat{T}(\epsilon_n) \end{aligned} \quad (13)$$

where $q = (\mathbf{q}, \epsilon_n)$ and $k = (\mathbf{k}, \omega_l)$. We will show the significant role of the VC given by the second term; $(\hat{L}^{\text{imp}} - \hat{O})$.

First, we study the impurity effect on the bare-bubble $\chi^{(0)}(k)$ for the $O_{x^2-y^2}$ quadrupole. The impurity effect is divided into the (i) self-energy correction (12) and (ii) vertex correction (13). If only (i) is taken into account, the bare-bubble within the d_{xz} -orbital is given as

$$\chi^{(0),\Sigma}(k) = -T \sum_{\mathbf{q}} G_{2,2}(k+q) G_{2,2}(q) \quad (14)$$

where G includes the self-energy, and the suffix 2 in G represents the d_{xz} -orbital. If both (i) and (ii) is taken into account, it is given as

$$\chi^{(0),\text{true}}(k) = -T \sum_{q, m, m'} \hat{L}_{m, m'}^{\text{imp}}(k; \epsilon_n) G_{m', 2}(k+q) G_{2, m}(q)$$

for $\hat{O} = \hat{O}_{x^2-y^2}$ in Eq. (13), where $l, m = 1 \sim 5$ represents the d -orbital. $\chi^{(0),\text{true}}$ gives the correct susceptibility for $n_{\text{imp}} > 0$, whereas $\chi^{(0),\Sigma}$ is incorrect.

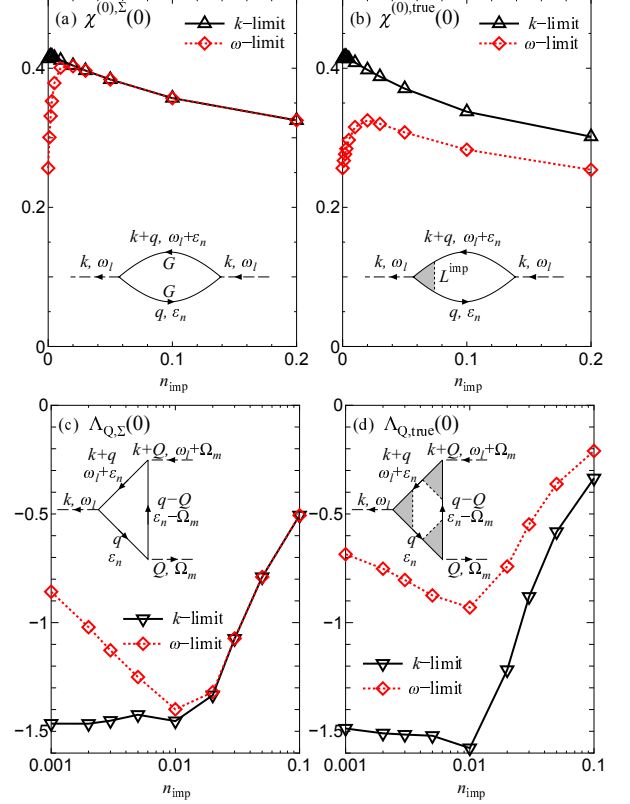


FIG. 5: (color online) (a) $\chi_{k(\omega)\text{-lim}}^{(0),\Sigma}$, (b) $\chi_{k(\omega)\text{-lim}}^{(0),\text{true}}$, (c) $\Lambda_{\mathbf{Q},\Sigma}^{k(\omega)\text{-lim}}$, and (d) $\Lambda_{\mathbf{Q},\text{true}}^{k(\omega)\text{-lim}}$ as functions of n_{imp} . The correct results are given in (b) and (d). Here, ω -limit values are obtained by extrapolating the data at ω_l with $l = 1 \sim 10$ to the real axis numerically.

Here, we discuss the susceptibilities in the k -limit and ω -limit. Using Eq. (14) or (15), the former is simply given as $\chi_{k\text{-lim}} = \chi(\mathbf{k}, \omega_l)$ at $l = 0$ and $\mathbf{k} = 0$. Here, we derive the latter numerically by extrapolating the data at ω_l with $l = 1 \sim 10$ to the real axis. This procedure is successful at sufficiently low temperatures. Figure 5 (a) and (b) represent the numerically obtained $\chi_{k(\omega)\text{-lim}}^{(0),\Sigma}$ and $\chi_{k(\omega)\text{-lim}}^{(0),\text{true}}$ for $I = +1$, respectively. We fix $T = 3$ meV and $n = 6.0$. In (a), $\chi_{\omega\text{-lim}}^{(0),\Sigma}$ quickly increases with n_{imp} , and it is almost equal to $\chi_{k\text{-lim}}^{(0),\Sigma}$ just for $n_{\text{imp}} \gtrsim 0.01$. In (b), in contrast, $\chi_{\omega\text{-lim}}^{(0),\text{true}}$ does not reach the k -limit value even for $n_{\text{imp}} \sim 0.1$. In both (a) and (b), impurity effect on the k -limit value is very small. Since $\chi_{k(\omega)\text{-lim}}^{(0),\text{true}}$ gives the true susceptibility, we conclude that the relationship $\chi_{k\text{-lim}}^{(0)} > \chi_{\omega\text{-lim}}^{(0)}$ is satisfied even for $n_{\text{imp}} > 0$.

In Fig. 5 (a), $\chi_{\omega\text{-lim}}^{(0),\Sigma}$ approaches to the k -limit value

for $n_{\text{imp}} > 0$, since the intra-band Pauli term also contributes to the ω -limit ($\mathbf{k} = 0$ and $\omega \rightarrow 0$) due to the broadening of the quasiparticle spectrum caused by $\text{Im}\Sigma$. However, the impurity three-point vertex $\hat{L}^{\text{imp}}(k; \epsilon_n)$ takes large value for $\omega_l \cdot (\epsilon_n + \omega_l) < 0$, and it suppresses the Pauli term. These effects exactly cancel for conserved quantities: For this reason, the charge and spin susceptibilities become zero in the ω -limit even for $n_{\text{imp}} > 0$. Although $O_{x^2-y^2}$ is not conserved, the VC in $\hat{L}^{\text{imp}}(k; \epsilon_n)$ is nonzero in the present model, and therefore the relationship $\chi_{k\text{-lim}}^{(0),\text{true}} > \chi_{\omega\text{-lim}}^{(0),\text{true}}$ is satisfied.

Next, to discuss the AL-VC, we calculate $\Lambda_{\mathbf{Q}}^{k(\omega)\text{-lim}}$ at $\mathbf{Q} = (0, \pi)$ introduced in the main text (Eq. (8)) in the presence of impurities ($I = +1$), by which the AL-VC is given as $X_{k(\omega)\text{-lim}} \sim T|\Lambda_{\mathbf{Q}}^{k(\omega)\text{-lim}}|^2 \sum_{\mathbf{k}} \chi^s(\mathbf{k})^2$. Figure 5 (a) shows the numerically obtained $\Lambda_{\mathbf{Q},\Sigma}^{k(\omega)\text{-lim}}$, in which only Σ^{imp} is included. We see that $\Lambda_{\mathbf{Q},\Sigma}^{k(\omega)\text{-lim}}$ increases with n_{imp} , and coincides with the k -limit value just for $n_{\text{imp}} \gtrsim 0.01$. We also calculate $\Lambda_{\mathbf{Q},\text{true}}^{k(\omega)\text{-lim}}$, in which both Σ^{imp} and L^{imp} are taken into account properly. In this case,

$\Lambda_{\mathbf{Q},\text{true}}^{\omega\text{-lim}}$ does not reach the k -limit value even for $n_{\text{imp}} \gtrsim 0.1$ thanks to the VC in L^{imp} . Since $\Lambda_{\mathbf{Q},\text{true}}^{k(\omega)\text{-lim}}$ gives the true vertex function, the relation of the AL-VC $X_{\text{true}}^{k\text{-lim}} > X_{\text{true}}^{\omega\text{-lim}}$ is confirmed even for $n_{\text{imp}} > 0$.

In summary, we confirmed that the relationship $\chi_{k\text{-lim}} > \chi_{\omega\text{-lim}}$ is satisfied in the presence of impurities, by taking both Σ_{imp} and L^{imp} into account correctly. In other words, although the relation $\chi_{k\text{-lim}} \approx \chi_{\omega\text{-lim}}$ is obtained by including Σ_{imp} only, it is an artifact due to the neglect of the VC in L^{imp} . (Since $L^{\text{imp}} = \hat{O}$ for the charge current $\hat{O} = \mathbf{v}_{\mathbf{k}}$, such discontinuity will be absent for the conductivity.) In real compounds, the Raman vertex $\hat{R}_{x^2-y^2}$ is very complex and momentum dependent. In this paper, we take the momentum average of $R_{x^2-y^2}^{l,l}$ ($l = 2, 3$), and consider the constant Raman vertex $\hat{O}_{x^2-y^2}$ to simplify the discussion. In the present multiorbital model, L^{imp} does not vanish even if the \mathbf{k} -dependence of $\hat{R}_{x^2-y^2}$ is taken into account, so the relationship $\chi_{k\text{-lim}} > \chi_{\omega\text{-lim}}$ should be satisfied for $n_{\text{imp}} > 0$.